Scientific Research Publishing

Journal of Applied Mathematics and Physics, 2025, 13(10), 3596-3615
https://www.scirp.org/journal/jamp
ISSN Online: 2327-4379
ISSN Print: 2327-4352

The Quantum-Mechanical Explanation of the Thermal Radiative Behaviour of Helium

Thomas Allmendinger

Glattbrugg, Switzerland
Email: inventor@sunrise.ch

How to cite this paper: Allmendinger, T. (2025) The Quantum-Mechanical Explanation of the Thermal Radiative Behaviour of Helium. *Journal of Applied Mathematics and Physics*, **13**, 3596-3615.
https://doi.org/10.4236/jamp.2025.1310201

Received: September 20, 2025
Accepted: October 28, 2025
Published: October 31, 2025

Abstract

In order to apply the recently published planar atom model of Helium with well-defined electron trajectories onto the results about the thermal radiative behaviour of gases, which was published by the author in 2016, the latter publication had to be partly questioned since its theoretical evaluation contains several errors. Nevertheless, the basic statements made therein, applying the kinetic gas theory, are still valid. Since they cannot be assumed as commonly known, first, the description of the measurement equipment and the applied light sources, the most relevant results, and the basic theoretical interpretation were recapitulated. The essential empirical result of those measurements was the observation that any gas is warmed up when it is thermally irradiated, but solely up to a *limiting temperature* where the absorption intensity of the gas is equal to its emission intensity. This effect was first observed in air and in CO_2, whereby the limiting temperatures were nearly equal. But it also occurred in the noble gases Argon, Neon and Helium, whereby the limiting temperatures depended on the type of gas. These differences could be explained by means of the kinetic gas theory, assuming proportionality between the *collision wattage* of the atoms and the *radiation wattage*. As a consequence, an *additional energy* must exist, which does not appear in the classic thermodynamic theory, and which must be due to an *oscillating process* at the electrons. In order to explain this, using the example of Helium, the said atom model is adduced. Since it exhibits well-defined electron trajectories—in contrast to the orthodox orbital model where the electrons underlie probabilities of presence—such an oscillation process, implicating an excited state of the electrons, is well describable. Thereto, a modified *harmonic oscillator* comes into question. This oscillator is *eccentric* since it rotates around the nucleus. Moreover, it is *asymmetric* since its energetic conditions are asymmetric with respect to the orbit path. In particular, the quantum-mechanical condition of a *standing wave* must be fulfilled, *i.e.* the angular velocity ω_{osc} of the oscillator must be an integer multiple of the angular rotation velocity ω_{rot}, preferably 2. By equating the oscillation energy

of the electrons and the radiation energy, which is determined by Einstein's equation for the photoelectric effect, and by applying the *theorem of conservation of momentum* ***P*** onto the collision process, thermodynamics could be bridged with quantum mechanics, delivering in the excited state an elliptic orbit. The essential difference between the orthodox and the alternative model consists in the fact that the orthodox model only considers the observers' point of view, whereas the alternative model distinguishes between object and observer. Thereby, the isolated model is two-dimensional, obeying the here described quantum mechanical computation, whereas from the viewpoint of the observer, it is three-dimensional, due to the thermally induced rotation.

Keywords

Kinetic Gas Theory, 2D-Atom Model of Helium, Thermal Radiation Absorption and Emission by Gases, Electronic Oscillation, Bridge Thermodynamics/Quantum-Mechanics

1. Introduction

The adsorption and the emission of thermal radiation by gases both play a major role in atmospheric physics, in particular with respect to climate change, which is commonly ascribed to the increase of CO_2 in the atmosphere. In order to describe the thermal radiation intensity Φ of the atmosphere (measured in Wm^{-2}), the *Stefan-Boltzmann Relation* is applied, which expresses coherence with the absolute temperature according to $\Phi = \sigma \cdot T^4$ (σ = Stefan-Boltzmann constant). This relation was established at the end of the 19th century [1] [2], being derived from laboratory measurements made by Dulong and Petit in the first quarter of the 19th century [3]. In fact, it concerns *Black Bodies*, implying radiation and counter-radiation, but it seems also applicable to the atmospheric radiation, using Equation (1):

$$\Phi_{solar} \cdot (1-\alpha) = \sigma \cdot \left(T_{surf}^4 - T_{amb}^4\right) \tag{1}$$

where α = colour-dependent reflection coefficient;

T_{surf} = temperature of the Earth surface or of an opaque body at the Earth surface;

$T_{ambient}$ = temperature of the ambient atmosphere.

Even though Equation (1) delivers plausible results for solar heat collectors, it may be a fallacy, due to an accidental coincidence of the atmospheric behaviour with that of a Black Body, since its absorption behaviour does not at all correspond to the absorption behaviour of a Black Body (which is by definition total). Moreover, this relation does not describe the temporal occurrence of this equilibrium state. But in particular, it appears strange that the radiation of a gas (air) would solely depend on the temperature and not on the pressure, too.

Nevertheless, it was incorporated into the atmosphere theory by Arrhenius [4],

describing the counter-radiation of the atmosphere against the Earth surface. Thereby, the additional fault was made by referencing it to the Space-temperature, whereby $T_{Space} = T_{amb} = 0$ K (or strictly speaking 2.7 K), thus disregarding the complex influence of the intermediate atmosphere.

This approach is in principle still in use (see, e.g. [5]). Thereby, several theories exist about the so-called *radiative heat transfer* between Earth surface and Space, implicating the assumption that the atmosphere radiates like a Black Body, and applying the Stefan-Boltzmann Relation. But they disregard the fact that this relation is solely valid under conditions of equilibrium, and in particular that in this regard, the so-called greenhouse gases, such as CO_2, which are generally blamed for climate change, do not occur. Furthermore, apart from the fact that the CO_2-concentration is very low (namely about 400 ppm = 0.04%), according to **Figure 1**, the spectrum of solar light loses intensity over its whole—also visible—range, due to absorption by the atmosphere. However, the citation of the diagram depicted in **Figure 1** could not be found. At all, the wave-length-specific light intensity would not be easily detectable. Nevertheless, the considerable intensity difference of sunlight between the extra-terrestrial position and the position at the Earth surface is evident and measurable.

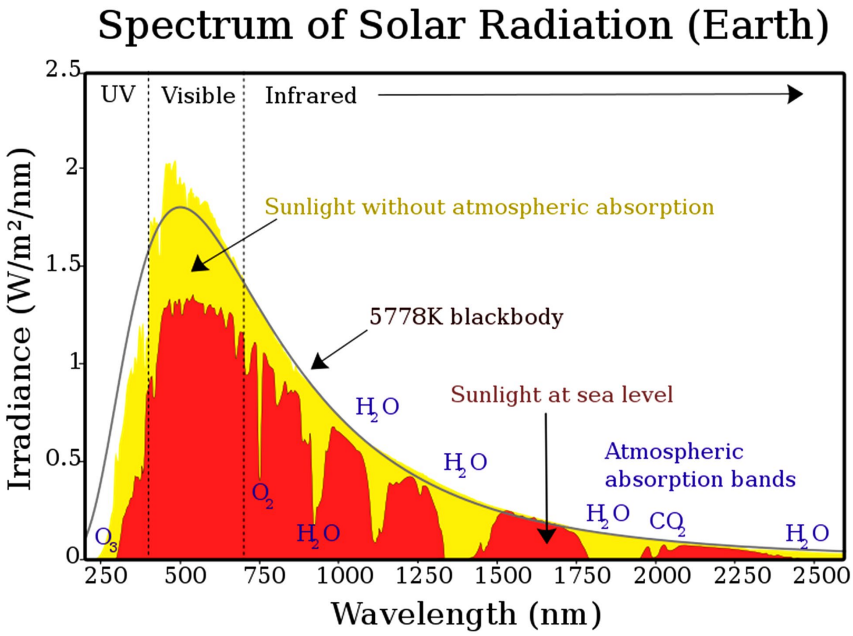

https://en.wikipedia.org/wiki/Solar_irradiance#/media/File:Solar_spectrum_en.svg.

Figure 1. Solar irradiance spectrum above atmosphere and at surface.

A further but significant problem arises from the difficulty in transferring photometric or spectroscopic data to the behaviour of thermally irradiated gases. In fact, there is no coherence between the respective results—originally delivered by Tyndall in 1860 [6], and later ascertained by IR-spectra—and the warming-up temperature of gases.

Consequently, no method for measuring the warming-up of a thermally irradiated gas existed, and it was not evident that this warming-up is due to vibrations of the molecular bonds which are associated with the absorption of infrared rays. Rather, the hypothesis emerged that another cause could be linked to the ability of gases to absorb and emit thermal radiation, namely the *oscillation of the atomic electron shell*. This proved to be all the more true when the own results, first published in 2016 by the author [7], revealed that *any* gas can absorb and emit thermal radiation, even the noble gases.

The therein described measurements were made using tubes by Styrofoam, which exhibits a low heat-capacity, minimizing the interference between gas and tube. The measuring equipment and the most important results are recapitulated in Chapter 2. The essential, so far nowhere reported phenomenon was the fact that an irradiated gas attains after a certain time a *limiting temperature* where the absorption intensity is equal to the emission intensity.

Similar results for air, carbon-dioxide and Argon were independently reported by Seim and Olsen in 2020 [8], but without an evaluation in the same manner. Besides, the influence of thermal radiation on the thermal behaviour of gases was not considered so far, solely the collision-induced *spectral absorption* (CIA). It was discovered in 1949 by Crawford and co-workers for forbidden vibrational transitions in compressed O_2 and N_2 gases (so-called super-molecular systems) [9]. Till 1993, 800 original papers were published in the field, also including noble gas mixtures [10]. Since then, further papers appeared, e.g. [11]. But a direct correlation between spectral absorbance and thermal behaviour of gases does not exist.

Based on the empiric results given in [7], an explanation was given using the *kinetic gas theory*, which connects the heat content of a gas to the kinetic translation energy of its particles (molecules or atoms). And indeed, a correlation was found between the *collision wattage* and the *radiation wattage*. Thereby, the different limiting temperatures of Argon, Neon and Helium could be explained.

However, its theoretical explanation was not feasible since thermal radiation does not occur in thermodynamics. But obviously, an *additional energy* must exist which is responsible for the electromagnetic radiation, acting as transformer. The only possible cause is an *oscillation or pulsation of the electronic shell* of the (noble gas) atoms, obeying quantum-mechanical criteria.

And thereto, the recently published atom model of Helium with well-defined planar electron trajectories [12] comes into question, namely by applying an eccentric oscillation process onto the electron rotation and regarding the standing wave condition.

The key principle of that model consists in the hypothesis that both electrons which diametrically circle round the nucleus obey the conservation of momentum $\hbar$ ($=h/2\pi$). But since their partial three-dimensional pathways proceed orthogonally, the resulting mutual pathway is two-dimensional, exhibiting the angular momentum $\sqrt{2}\hbar$ (see **Figure 2**).

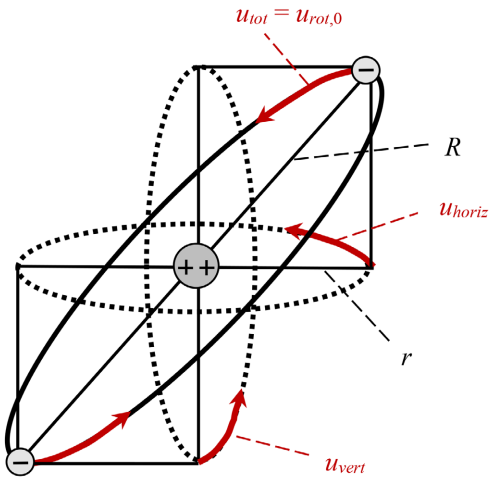

Figure 2. 2D-model of Helium composed by two imaginary orthogonal orbits of the electrons, according to [11].

This model is two-dimensional. However, it describes an isolated Helium atom in the ground state. In reality, each atom is part of a gas, being in translation as well as in rotation move. And as a consequence of the latter one, it apparently becomes three-dimensional. Thereby, the stochastic thermodynamics—particularly the kinetic gas theory—and the exact quantum mechanics can be bridged theoretically. This is subject of the following chapters.

2. Recapitulation of the Measurements and of the Applied Kinetic Gas Theory

The respective measurements described in [7] were carried out by means of one-meter-long quadratic tubes from Styrofoam using sunlight (**Figure 3**) as well as artificial light (**Figure 4**), whereby the light source was positioned at the top. In order to measure the temperature course, three thermometers were mounted at three positions.

Figure 3. Solar tube.

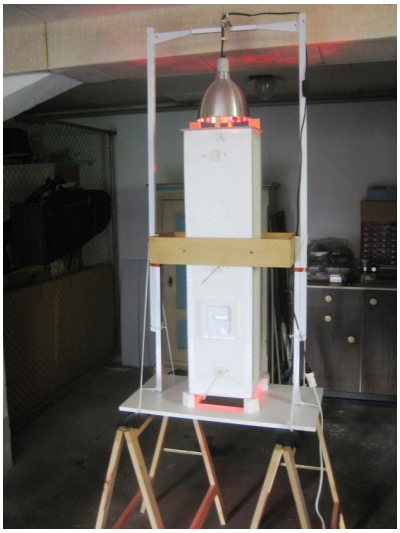

Figure 4. Heat radiation tube.

The experimental difficulties and the instrumental optimizations are discussed in [7]. The largest difficulty consisted in the fact that the intensity of artificial light decreases inversely proportional to the square of the distance, even if no absorption occurs. That became apparent while—in the cases where artificial light was used—at the different measuring points, temperature differences arose (Figure 5), whereas that was not the case when sunlight was used (Figure 6). In any case, the temperature ascent began simultaneously at the three thermometer positions, which delivered evidence that the warming-up was induced by thermal radiation and not by thermal conductivity.

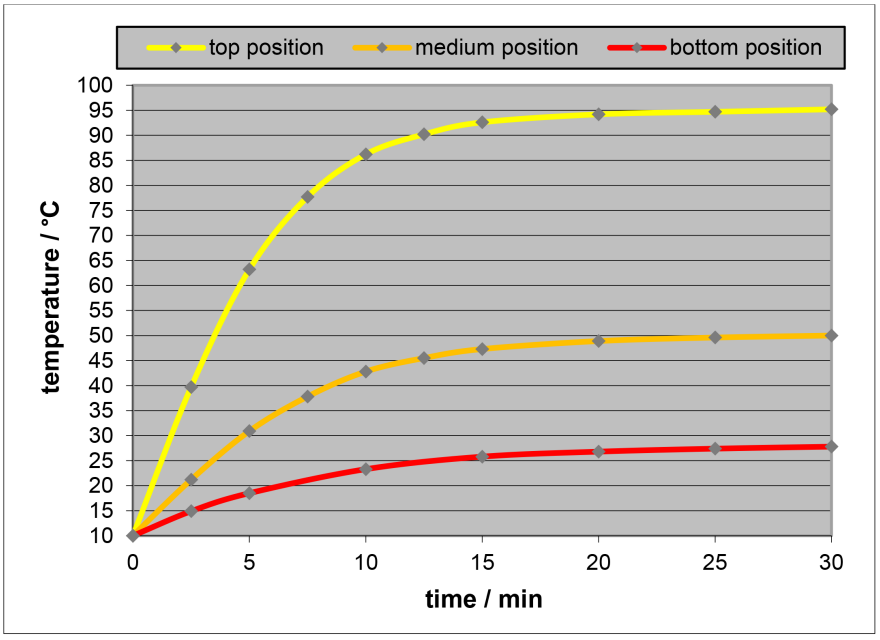

Figure 5. Heat radiation tube (not optimized), filled with air, 150 W IR-spot: Temporal courses at the three thermometer positions (Figure 9 in [7]).

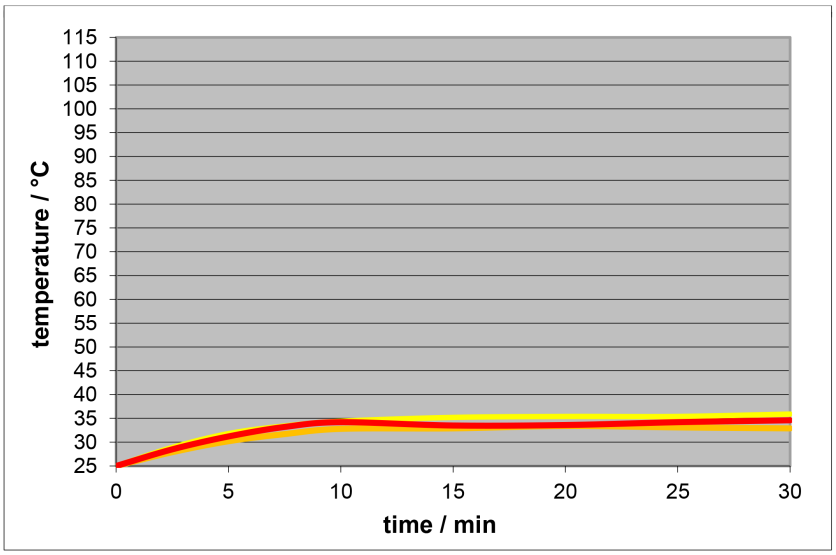

Figure 6. Outdoor solar-tube, filled with air, irradiation wattage 1000 Wm^{-2} (measured by an electronic pyranometer): Temporal courses at the three thermometer positions (Figure 20 in [7]).

Initially focused on CO_2, which is pivotal for the current climate-change theory, and which was the inducement for these measurements, the investigations were extended to other gases, firstly to air and an artificial Nitrogen/Oxygen 4:1 mixture. Surprisingly, they exhibited a quite similar behaviour as pure CO_2 (Figure 7). But even noble gases turned out to be active, namely in such a way: When a gas is thermally irradiated, it is warmed up till a *limiting temperature* is reached where the absorption intensity of the gas (measured in Wm^{-2}) is equal to its emission intensity. Therefore, it can be concluded that *any* gas is not only able to *absorb* but also to *emit* thermal radiation. However, the limiting temperature depends on the gas type, e.g. it is lower for Helium than for Argon (Figure 8).

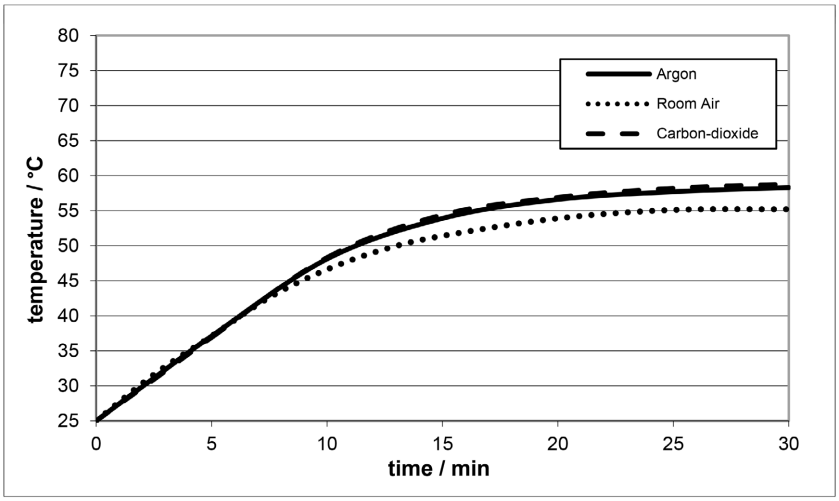

Figure 7. Average warming-up rates for different gases, measured by the heat radiation tube (method A, 150W IR-spot, medium thermometer position) (Figure 25 in [7]).

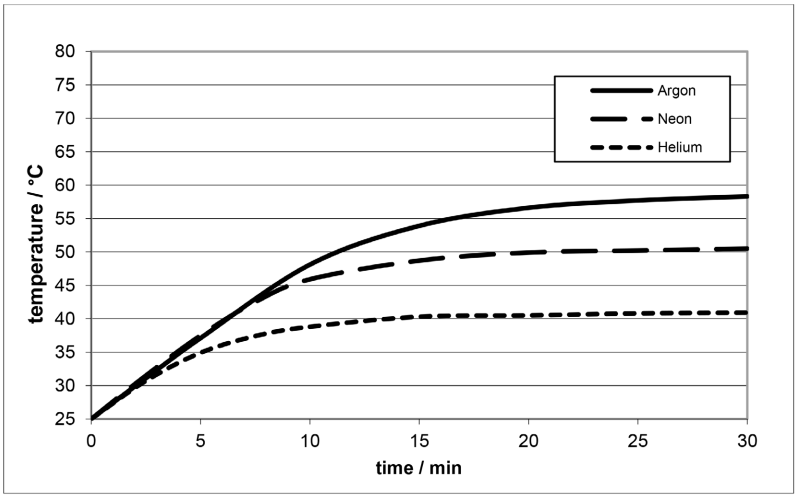

Figure 8. Average warming-up rates for different gases, measured by the heat radiation tube (method A, 150W IR-spot, medium thermometer position) (Figure 26 in [7]).

As already mentioned, these differences could be explained by applying the kinetic gas theory, which assumes correlation between the average kinetic translation energy of the particles (molecules or atoms) and the absolute temperature, according to Equation (2):

$$\overline{E}_{kin,atom} = \frac{1}{2} m \overline{w}^2 = \frac{3}{2} k_B T \tag{2}$$

where m = mass of a single particle (atom or molecule) = molar atom mass M/N_A;

N_A = Avogadro Constant = 6.022×10^{23};

$\overline{w}$ = average velocity of this particle;

k_B = Boltzmann Constant = 1.381×10^{-23} J·K^{-1};

T = absolute temperature.

This approach is based on the assumption of the molar heat capacity with constant volume $C_V = 3/2R$ (which is equal for all noble gases). Instead, the heat capacity with constant pressure $C_p = 5/2R$ could be used. In the present case, both conditions seem to be fulfilled, namely constant volume as well as constant pressure. However, the respective volume is insofar not constant as the measuring tube is not perfectly tight. Thus, in fact, a medium case exists which appears not being exactly describable.

Based on this and regarding the cross-sectional area σ of the atom, the average collision frequency $\overline{z}$ [s^{-1}] can be deduced (Equation (3)), yielding, in combination with the kinetic energy, the *kinetic collision wattage* $\overline{P}_{kin,atom}$ of each atom (Equation (4)):

$$\overline{z} = \frac{\overline{w} \cdot \sigma \cdot p \cdot \sqrt{2}}{k_B \cdot T} \tag{3}$$

$$\overline{P}_{kin,atom} = \overline{P}_{collision} = \overline{E}_{kin,atom} \cdot \overline{z}_{atom} = 3p \cdot \sigma \cdot \sqrt{\frac{3RT}{2M}} \tag{4}$$

where p = pressure [1 bar = 10^5 Pa = 10^5 kg·m^{-1}·s^{-2}];

σ = cross sectional area of the atom = $r^2 \cdot \pi$ (r = atomic radius);

R = universal gas Constant = $k_B \cdot N_A = 8.314\ \mathrm{J \cdot K^{-1} \cdot mol^{-1}}$;

M = molar atom mass [$\mathrm{kg \cdot mol^{-1}}$] = $m \cdot N_A$.

When comparative measurements are made under the same conditions (same apparatus, same light source, same pressure), the following relation (5) is valid, making use of the limiting temperatures T_{lim}:

$$r_2 / r_1 = \sqrt[4]{\left(M_2 / M_1\right) \cdot \left(T_{lim,1} / T_{lim,2}\right)} \tag{5}$$

For the noble gases Helium, Neon and Argon, the following plausible atomic radii are obtained:

$$r_{\mathrm{Ar}} = (\text{assumed}) 1 \times 10^{-10}\ \mathrm{m}\ \ (=1\ \text{Å}) \qquad r_{\mathrm{Ne}} = 0.85 \times 10^{-10}\ \mathrm{m} \qquad r_{\mathrm{He}} = 0.57 \times 10^{-10}\ \mathrm{m}$$

The pressure dependency of the atmospheric radiation intensity according to Equation (4) could be demonstrated by later experiments, carried out at different altitudes in order to vary the atmospheric pressure, and described in [13]. By the thereby applied method, described in [14], the temperature rise of differently coloured aluminium-plates is measured when they are exposed to solar radiation. Similarly to the case of irradiated gases, in the case of irradiated opaque plates, after a certain time, a limiting temperature is attained whereby the—colour-dependent—absorbed solar radiation is in equilibrium with the—colour-independent—thermal radiation of the plates and the counter-radiation of the atmosphere. However, the time needed to attain the limiting temperature is much longer than in the case of gas-irradiation, namely several hours. The different altitudes implicated different atmospheric pressures, light intensities and temperatures. The thereby measured value for the *atmospheric emission constant A* was 22 $\mathrm{Wm^{-2} \cdot bar^{-1} \cdot K^{-0.5}}$, delivering the thermal radiation intensity $\Phi = A \cdot p \cdot T^{0.5}$.

The respective principal assumption consists of a correlation between the collision-wattage and the radiation-wattage, expressed by the *transformation coefficient* ε:

$$\overline{P}_{radiation} = \overline{P}_{emission} = \varepsilon \cdot \overline{P}_{collision} \tag{6}$$

Thereby, the considerable problem arises that the determinable radiation wattage is normally related to area ($\mathrm{Wm^{-2}}$), whereas Formula (4) is related to a single atom, enabling the computation of a volume-related value since the general gas law delivers the coherence between particle number and volume.

This problem could not be satisfyingly solved in [7]. Therefore, a spatial particle model was developed corresponding to a close-packing of equal spheres, as it is usual in crystallography. But since it does not affect the essential objective of this treatise, it is omitted here. Rather, the application of the here used atom model is described next.

3. The Eccentric Asymmetric Harmonic Oscillator

As scheduled in **Figure 9**, the radiation emitted by a spot (or by another light-source which comprises thermal radiation) can be absorbed by atoms which un-

dergo an electronic excitation being able either to emit thermal radiation or to increase the heat content. Conversely, the kinetic heat of the gas leads to an excited state. When the limiting temperature is reached, the heat-content of the gas cannot be increased furthermore, so that the absorption intensity becomes equal to the emission intensity.

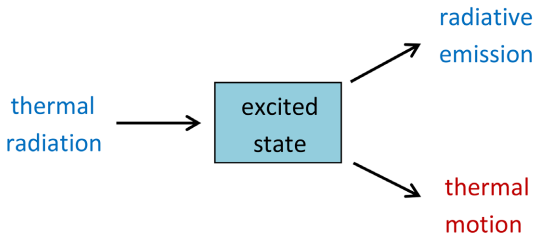

Figure 9. Schema of the energetic relations at the atom.

As a consequence, an electronically excited state of the atom must exist, which implies an energetic elevation. It is characterized by an electronic oscillation that is able to transfer the oscillation energy to kinetic motion as well as to electromagnetic radiation. And this can be modelled by means of an *eccentric asymmetric harmonic oscillator*, using the recently published planar atom model of Helium [12], already roughly described in Chapter 1. The values of the parameters for this model in the ground state are:

$$R_0 = 0.5644\times10^{-10}\ \text{m} \qquad u_{rot,0} = 2.901\times10^{6}\ \text{m}\cdot\text{s}^{-1} \qquad \omega_0 = 5.14\times10^{16}\ \text{s}^{-1}$$

Using this model, an *excited electronic state* can be supposed which enables absorption as well as emission of electromagnetic radiation, but which—beyond that—is capable to transfer kinetic energy to another atom. And as it would seem obvious, the energy of the excited state should have the character of an *eccentric oscillation*, superimposed on the rotation of the electrons, and in combination with the rotation, inducing a *pulsation*.

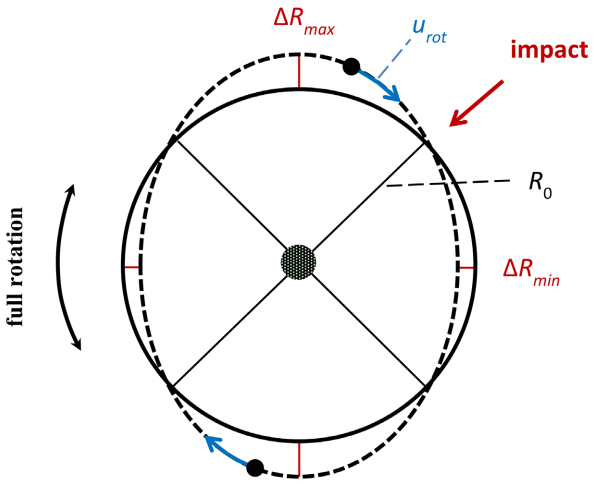

Figure 10. Orbit of the electrons as a result of a collision or a thermal-radiative excitation (= dotted curve; red lines: maximal and minimal positions of the electrons).

This constellation is scheduled for $\omega_{osc} = 2\omega_{rot}$ in Figure 10, expressing a standing wave. Thereby, it has to be regarded that, due to heat motion, the atoms are not immobile. Rather, they move not only in the form of translation but also in the form of rotation (here called *full rotation*), which both are not quantised. Thus, viewed from the position of an outside observer, the atom appears to pulsate in all directions due to the oscillation of the electron orbit.

In contrast, within the atom, the conditions are strictly defined. And since the orbital angular momentum must be constant, the rotation velocity u_{rot} as well as the angular velocity ω_{rot} depend on the rotation radius R (see Equation (7)):

$$u_{rot} \cdot R \cdot m_e = \omega_{rot} \cdot R^2 \cdot m_e = \sqrt{2} \cdot \frac{h}{2\pi} \rightarrow \omega_{rot} = \sqrt{2} \cdot \frac{h}{2\pi} \cdot \frac{1}{R^2 \cdot m_e} \tag{7}$$

Regarding this, it suggests itself to assume an *asymmetric harmonic oscillator* which can be mathematically formulated by Equation (8) and illustrated in Figure 11.

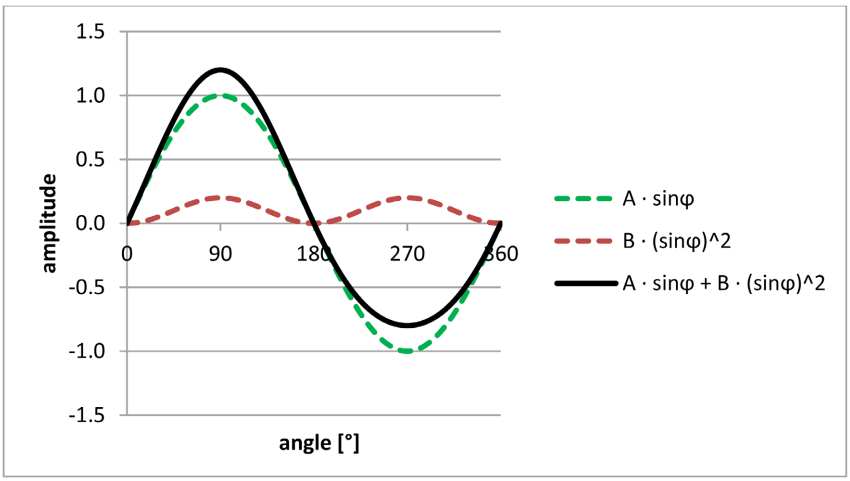

Figure 11. General description of an asymmetric harmonic oscillator.

$$\Delta R = A \cdot \sin\varphi + B \cdot (\sin\varphi)^2 \tag{8}$$

ΔR = distance deflexion

$$A = (\Delta R_{max} + \Delta R_{min})/2$$

$$B = (\Delta R_{max} - \Delta R_{min})/2$$

$$\varphi = \omega_{osc} \cdot t$$

However, this approach is not strictly correct since—as mentioned above—ω_{rot} is not constant. Nevertheless, it seems advisable to make such an approximation by assuming ω_{rot} as constant and u_{rot} as variable in order to give a basic idea of the whole process. Thereby, the boundary condition must be observed that ω_{osc} has to be in a distinct ratio to $\omega_{rot,0}$ in order to enable a standing wave condition. In the simplest case, ω_{osc} is twice as big as $\omega_{rot,0}$. In principle, other ratios are possible, but they are disregarded here.

As for any harmonic oscillator, the total energy of an asymmetric harmonic oscillator is given by the *kinetic energy of the oscillating electrons at the turning-over point*, *i.e.* at the point where the distance deflexion as well as the potential energy is zero. And since two diametrically running electrons are implied, its double amount must be used.

As already mentioned—or rather approximately assumed—both angular velocities (ω_{rot} and ω_{osc}) are considered as constant. Consequently, the oscillation velocity u_{osc} results from the mathematical derivation of the distance deflexion ΔR (given by Equation (8)) and becomes a function of time, expressed by Equation (9):

$$u_{osc} = \Delta\dot{R} = A \cdot \omega_{osc} \cdot \cos\left(\omega_{osc} t\right) + 2B \cdot \omega_{osc} \cdot \cos\left(\omega_{osc} t\right) \cdot \sin\left(\omega_{osc} t\right) \tag{9}$$

This yields at the turning-over point where $\omega_{osc} \cdot t$ = kinetic energy = total energy Equation (10):

$$E_{osc} = m_e \cdot \left(u_{osc,turn}\right)^2 = m_e \cdot A^2 \cdot \left(\omega_{osc}\right)^2 \tag{10}$$

where m_e = electron mass = 0.9109×10^{-30} kg;

A = amplitude, according to Equation (8).

But whereas ω_{osc} is given by the here used atom model, the amplitude A is not readily known. If it were known, the proportion of its parts ΔR_{max} and ΔR_{min} could be determined, as will be demonstrated in Chapter 5.

However, first of all, a relation between this electronic oscillation energy and the thermally induced kinetic energy has to be found. Thereto, Einstein's equation $E = h \cdot \nu_{rad}$ has to be regarded, being already presented in [7] but exhibiting considerable errors which are discussed in the next chapter.

Besides, in [7], the relevant frequency (or the respective wave length) was not precisely known but roughly estimated by comparing the results obtained by sunlight and by artificial light, using Planck's distribution law and the producer's specifications, yielding 1.9 μm. This value seems quite low since it is not far from the visible (red) light at 0.78 μm. Subsequent experiments with air and with CO_2 [15], using a hot-plate as thermal radiation source, mounted below, let suppose that higher electronic absorption (and emission) wave lengths are possible. However, an exact evaluation like the one applied in [7] was not possible.

4. The Bridge between Thermal Motion and Electronic Oscillation

In the fundamental publication [7], at least two significant errors were made when trying to establish a connection between the kinetic energy $E_{kin,atom}$, expressed by Equation (11), being identical with Equation (2):

$$\Delta E_{kin,atom} = \frac{3}{2} k_B \cdot \Delta T \tag{11}$$

and the radiation energy E_{rad}, expressed by Einstein's formula for the photoelectric effect:

$$E_{rad} = h \cdot \nu_{rad} \quad (12) \text{ with } \quad h = 6.626 \times 10^{-34} \text{ J} \cdot \text{s} .$$

Since $\nu_{rad} \cdot \lambda_{rad} = c_{light} = 3.0 \times 10^{8}$ ms^{-1}, ν_{rad} becomes 1.58×10^{14} s^{-1} when $\lambda_{rad} =$ 1.9 µm, while E_{rad} becomes 1.05×10^{-19} J.

In the first case, the absolute temperature $T = 300$ K was used instead of the temperature difference $\Delta T = T_{lim} - T_{amb}$, while in the second case, a calculation error was made by the factor of 1000.

But even when the corrected values are used, *i.e.* $\Delta T = 26$ K (according to Figure 12), the quotient $\Delta E_{kin}/\Delta E_{rad} = 5.4 \times 10^{-22}$ J/1.04×10^{-19} J = 5.2×10^{-3} (instead of 6.3×10^{-5} as indicated in [7]) is too low since it should be 1, which cannot be easily explained.

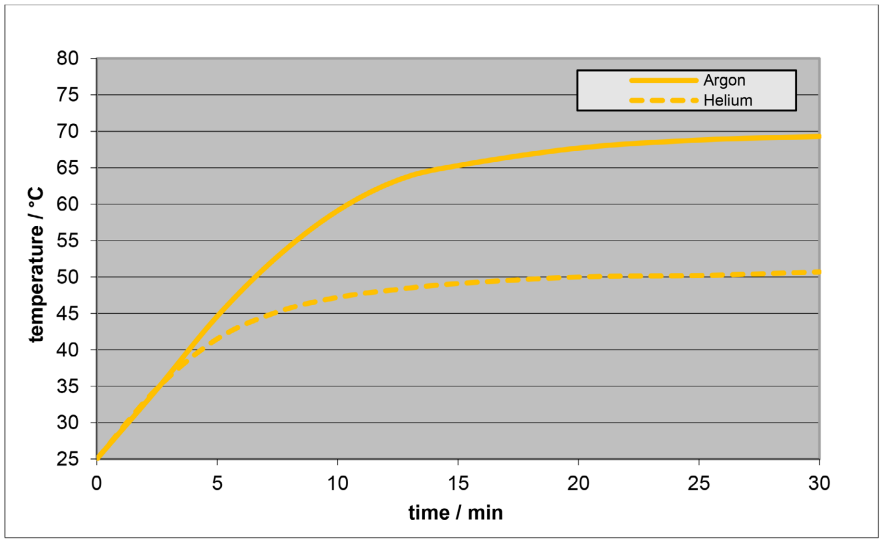

Figure 12. Comparison of Argon and Helium (method B2, 150 W, medium pos.) (Figure 27 in [7]).

A plausible explanation can be given by the previously described eccentric asymmetric harmonic oscillator, which is applicable on the planar atom model of Helium.

First of all, the model-specific expression for the oscillation energy according to Equation (10) can be compared with Einstein's expression for the radiation energy resulting in Equation (13), whereby the factor 1/2 is omitted since there are two electrons per atom:

$$E_{osc} = m_e \cdot \left(u_{osc}\right)^2 = m_e \cdot A^2 \cdot \left(\omega_{osc}\right)^2 = h \cdot \nu_{rad} \tag{13}$$

where m_e = electron mass = 0.9109×10^{-30} kg;

A = amplitude.

$$\omega_{osc} = 2\pi \cdot \nu_{osc} = 2\omega_0 = 10.28 \times 10^{16} \text{ s}^{-1}$$

In this equation, the two frequencies ν_{osc} and ν_{rad} occur, but not within the same mathematical power. Both are known (ν_{osc} according to the quantum mechanical supposition, and ν_{rad} according to the empirical estimation), while the unknown

parameter A exists. However, it can be computed using Equation (13). To verify it, regarding the uncertain character of ν_{rad}, an additional relationship based on the kinetic gas theory would be needed.

But even if such a relationship were not available, it is possible to assess its plausibility. Using the above parameters, the value obtained for A is 0.0327×10^{-10} m, which corresponds to 5.8 % of the atomic radius $R_0 = 0.5644 \times 10^{-10}$ m, appearing to be plausible. It also allows to compute the electron velocity at the turning-over point $u_{osc} = A \cdot \omega_{osc}$, yielding 0.336×10^6 m·s^{-1}. This value can be used for comparison with the kinetic gas theory.

Thereto, it seems obvious to apply the *theorem of conservation of momentum* $\boldsymbol{P}$ to the collision process, *i.e.* to the transfer of atomic motion to electronic motion, which is expressed by Equation (14):

$$\boldsymbol{P}_{electron} = m_e \cdot u_{osc} = \bar{\boldsymbol{P}}_{atom} = m_{\mathrm{He}} \cdot \Delta\bar{w}_{\mathrm{He}} \rightarrow u_{osc} = \frac{m_{\mathrm{He}}}{m_e} \cdot \Delta\bar{w}_{\mathrm{He}} \tag{14}$$

with $\Delta\bar{w}_{\mathrm{He}} = \sqrt{\frac{3k_B}{m_{\mathrm{He}}}} \cdot \left(\sqrt{T_{lim}} - \sqrt{T_{amb}}\right)$ according to Equation (2)

$$m_{\mathrm{He}} = 0.664 \times 10^{-26} \text{ kg}$$

$$m_e = 0.9109 \times 10^{-30} \text{ kg}$$

(In order to distinguish between both velocities, the different terms w (for the atoms) and u (for the electrons) are used).

Thereby, it has to be considered that $\sqrt{T_{lim}} - \sqrt{T_{amb}} \neq \sqrt{T_{lim} - T_{am}} = \sqrt{\Delta T}$.

But as Figure 13 reveals, within the range of the near-ground atmospheric temperature the two differences are proportional to one another, according to Equation (15):

$$\frac{\sqrt{T_{lim}} - \sqrt{T_{amb}}}{T_{lim} - T_{amb}} = 0.0277 \text{ K}^{-0.5} \rightarrow \sqrt{T_{lim}} - \sqrt{T_{amb}} = 0.0277 \text{ K}^{-0.5} \cdot \left(T_{lim} - T_{amb}\right) \tag{15}$$

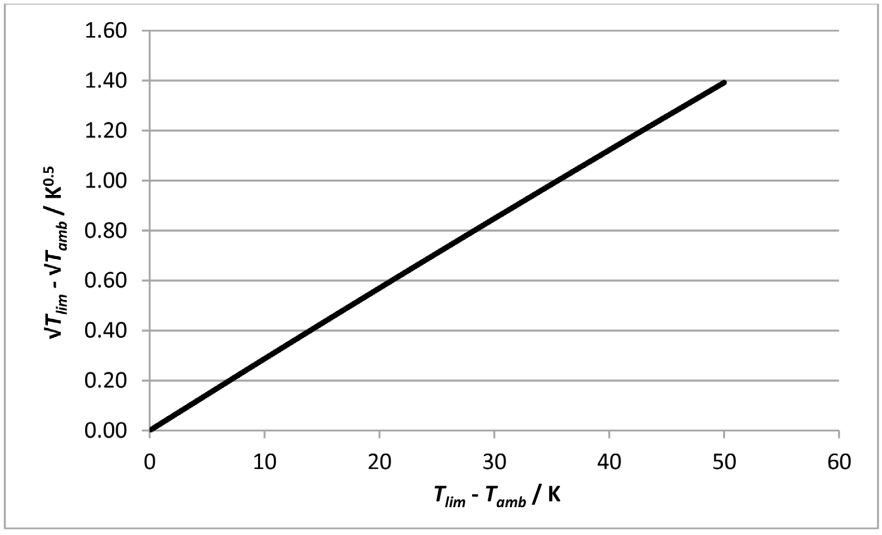

Figure 13. Plot of $T_{lim} - T_{amb}$ versus $\sqrt{T_{lim}} - \sqrt{T_{amb}}$.

Moreover, the temperature difference $\Delta T = T_{lim} - T_{amb}$ can be related to the area-related wattage of the spot by introducing the factor f according to Equation (16), which can be evaluated using a time-temperature diagram as the one depicted in Figure 12.

$$f = \frac{\Delta T}{\Phi_{apparent,area}} \rightarrow \Delta T = f \cdot \Phi_{apparent,area} \tag{16}$$

For Helium, f amounts to 0.0073 $Km^2 \cdot W^{-1}$, and when $\Phi_{apparent,area} = 3556\ Wm^{-2}$, ΔT_{He} becomes 26 K = 26˚C.

Using these relations, the values $A = 0.0355 \times 10^{-10}$ m and $E_{osc} = 0.121 \times 10^{-18}$ J are obtained, which yield for $\nu_{rad} = 1.83 \times 10^{14}\ s^{-1}$ and for $\lambda_{rad} = 1.67$ µm, being very close to the estimated value of 1.9 µm. Thus, the here used modelling method is in principle validated.

The energy conservation law appears not to be fulfilled here. However, this is due to the circumstance that two different energies are involved, namely the kinetic energy of the whole atom and the oscillation energy of the electrons, implying a splitting of the collision energy.

5. The Determination of the Asymmetric Parts at the Oscillator

In order to determine the maximal distances $R_{out} = R_0 + \Delta R_{max}$ and $R_{in} = R_0 - \Delta R_{min}$ of the two diametrically running electrons at the eccentric asymmetric harmonic oscillator, described by Equation (8), their energy contents have to be computed as a function of T and equated at their relevant value. Their energy contents are given by the sum of the potential energy and the rotation energy, while the oscillation energy E_{osc} is zero at these positions.

The *potential energy* can be computed using the expression for the Coulomb-force, which can be derived from Figure 11 and Formula (4) of [12], here designated as Formula (17):

$$F_{Coul} = \frac{15K}{8R^2} \rightarrow E_{pot} = \frac{15K}{8R} \tag{17}$$

where R = total radius between the nucleus and the electrons.

$$K = e^2 / 4\varepsilon_0 = 2.307 \times 10^{-28}\ J \cdot m$$

The computation of the *kinetic energy* requires the implementation of the angular momentum $\sqrt{2}\hbar = \sqrt{2}\, h/2\pi = 1.0546 \times 10^{-34}\ J \cdot s$ (which is characteristic for the here applied atom model of Helium) in order to determine the rotation velocity u_{rot} according to Equation (18):

$$u_{rot} = \sqrt{2} \cdot \frac{h}{2\pi} \cdot \frac{1}{R} \cdot \frac{1}{m_e} \tag{18}$$

$$m_e = 0.9109 \times 10^{-30}\ kg$$

Thereby, it has to be regarded that both electrons contribute to the kinetic energy, thus

$$E_{kin} = m_e \cdot (u_{rot})^2 = 2 \cdot \left(\frac{h}{2\pi}\right)^2 \cdot \frac{1}{R^2} \cdot \frac{1}{m_e} \tag{19}$$

Using these relations, the energies $\Delta E_{tot} = \Delta E_{pot} + \Delta E_{kin}$ can be computed for the outer position as well as for the inner position of the electrons, according to the Equations (20) - (22) and plotted as a function of the deflexion ΔR (Figure 14). Then, the ΔR-values which are relevant for E_{osc}, being determined in the previous chapter and amounting to 0.121×10^{-18} J, can be graphically determined, yielding 0.068×10^{-10} m for $\Delta R_{max,in}$ and 0.1035×10^{-10} m for $\Delta R_{max,out}$:

$$\Delta E_{pot,out} = \frac{15K}{8} \cdot \left[\frac{1}{R_0} - \frac{1}{R_0 + \Delta R_{out}}\right] \tag{20}$$

$$\Delta E_{pot,in} = \frac{15K}{8} \cdot \left[\frac{1}{R_0} - \frac{1}{R_0 - \Delta R_{in}}\right] \tag{21}$$

$$\Delta E_{kin,out} = 2 \cdot \left(\frac{h}{2\pi}\right)^2 \cdot \left[\frac{1}{(R_0 + \Delta R_{out})^2} - \frac{1}{R_0^2}\right] \tag{22}$$

$$\Delta E_{kin,in} = 2 \cdot \left(\frac{h}{2\pi}\right)^2 \cdot \left[\frac{1}{(R_0 - \Delta R_{out})^2} - \frac{1}{R_0^2}\right] \tag{23}$$

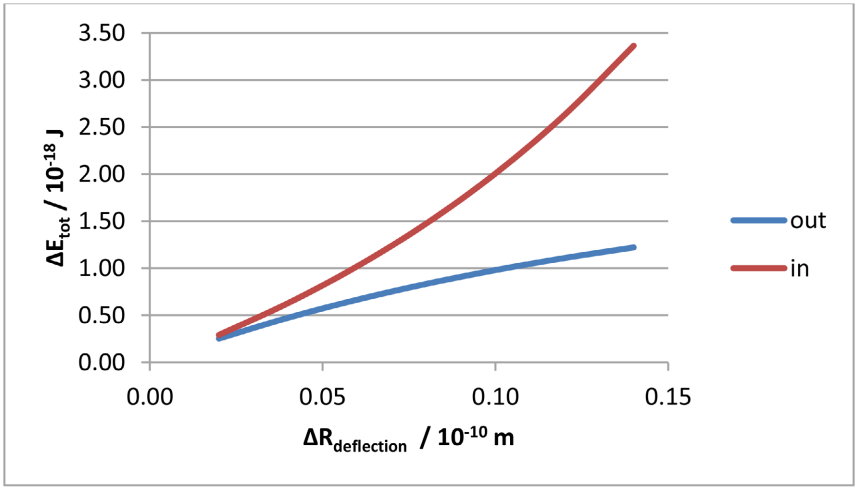

Figure 14. Plot of $\Delta R_{deflection}$ versus $\Delta E_{deflection,tot}$.

Based on these results, and approximately assuming that ω_{rot} and $\omega_{osc} = 2\omega_{rot}$ are constant, the calculation of the electron orbit in the excited state is possible, using Equation (8), and regarding that the rotation angle $\varphi = \omega_{rot} \cdot t$ (t = time), which implicates that $\omega_{osc} \cdot t = 2\varphi$. Thereby, the synonymous abbreviations $\Delta R_{max,in} \equiv \Delta R_{min}$ and $\Delta R_{max,out} \equiv \Delta R_{max}$ are assumed. As a consequence, the following values are obtained for the constants A and B:

$$A = \left(\Delta R_{max} + \Delta R_{min}\right)/2 = 0.08575 \times 10^{-10} \text{ m}$$

$$B = \left(\Delta R_{max} - \Delta R_{min}\right)/2 = 0.01775 \times 10^{-10} \text{ m}$$

The total radius of the electron orbit $R = R_0 + \Delta R$ (whereby $R_0 = 0.5644 \times 10^{-10}$ m) can be expressed by these constants and by the oscillating angle 2φ, according to Equation (24):

$$R = R_0 + A \cdot \sin 2\varphi + B \cdot (\sin 2\varphi)^2 \tag{24}$$

Now, the electron orbit can be expressed in Cartesian coordinates as follows:

$$x = R \cdot \sin \varphi$$

$$y = R \cdot \cos \varphi$$

which yields the relations (25a) and (25b):

$$x = \left[R_0 + A \cdot \sin 2\varphi + B \cdot (\sin 2\varphi)^2 \right] \cdot \sin \varphi \tag{25a}$$

$$y = \left[R_0 + A \cdot \sin 2\varphi + B \cdot (\sin 2\varphi)^2 \right] \cdot \cos \varphi \tag{25b}$$

and which is illustrated in Figure 15(a) and Figure 15(b), whereby the "ground state" means the non-excited equilibrium state at ambient temperature. They resemble the elliptic orbit shown in Figure 10 and thus confirm this approach, too.

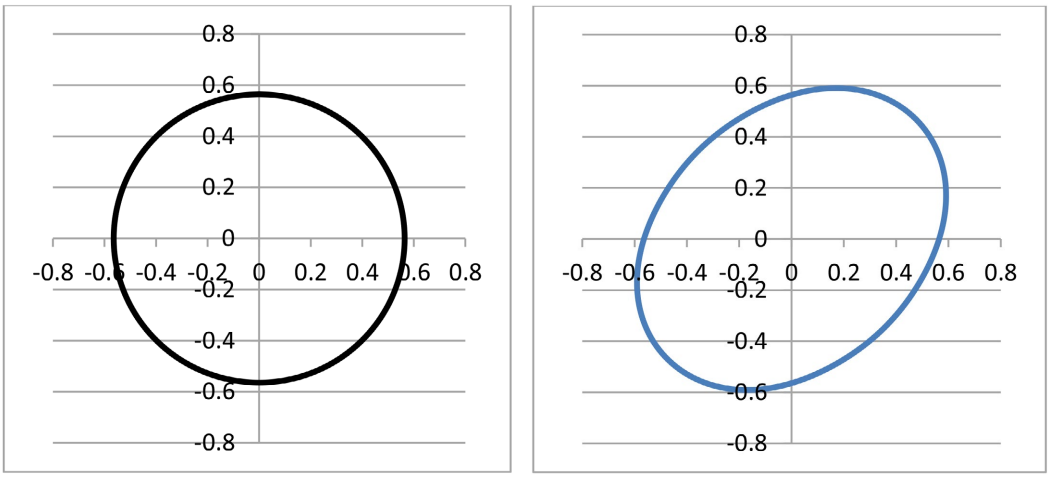

(a) (b)

Figure 15. (a) Orbit of the electrons in the ground state (units at both axis: 10^{-10} m); (b) Orbit of the electrons in the thermally excited state (units at both axis: 10^{-10} m).

6. Conclusions

In order to apply the recently published planar atom model of Helium [11] onto the results about the thermal behaviour of gases under the influence of infrared radiation, which was published by the author in 2016 [7], the latter publication had to be partly questioned since its theoretical evaluation contains several errors. Nevertheless, the basic statements made therein, applying the kinetic gas theory, are still valid. Since they cannot be assumed as commonly known, the description of the measurement equipment and the applied light sources (sunlight and IR-spot-light), the most relevant results, and the basic theoretical interpretation were

recapitulated in Chapter 2.

The essential empirical result of those measurements was the observation that any gas is warmed up when it is thermally irradiated, but solely up to a *limiting temperature* where the absorption intensity of the gas (measured in Wm^{-2}) is equal to its emission intensity. This effect was first observed with air (or a nitrogen/oxygen mixture) and with CO_2, whereby the limiting temperatures were nearly equal. But it also occurred at the noble gases Argon, Neon and Helium, whereby the limiting temperatures depended on the type of gas. These differences could be explained by means of the kinetic gas theory (which correlates the absolute temperature of a gas to the kinetic energy of the particles), assuming proportionality between the *collision wattage* of the atoms and the *radiation wattage*. Thereby, dependency of the radiation intensity on the gas pressure and on the absolute temperature was found.

As a consequence, an *additional energy* must exist, which does not appear in the classic thermodynamic theory, and which must be due to an oscillating process at the electrons. Hereto, solely a modified *harmonic oscillator* comes into question, preferably applied onto the simplest case—namely onto the planar atom model of Helium—and described in Chapter 3. This oscillator, illustrated in **Figure 10** and mathematically expressed by Equation (9), is *eccentric* since it rotates around the nucleus. Moreover, it is *asymmetric* since its energetic conditions are asymmetric with respect to the orbit path. In particular, the quantum-mechanical condition of a *standing wave* must be fulfilled, *i.e.* the angular velocity ω_{osc} of the oscillator must be an integer multiple of the angular rotation velocity ω_{rot}, preferably 2. But since the conservation of angular momentum $\sqrt{2}\hbar$ must be fulfilled, the difficulty arises that both angular velocities are not constant since they depend on the (variable) radius. In order to eliminate this difficulty, the approximation of a constant ω_{osc} was made, which delivered plausible results. Particularly, it implied an expression for the oscillation energy E_{osc} as a function of the electronic mass m_e, the amplitude A, and the angular velocity $\omega_{osc} = 2\omega_{rot}$:

$$E_{osc} = m_e \cdot A^2 \cdot \left(\omega_{osc}\right)^2 \tag{26}$$

which enables to compute A (if E_{osc} is known), or to compute E_{osc} (if A is known).

By equating the oscillation energy and the radiation energy, which was determined by Einstein's formula $E = h \cdot \nu_{rad}$, thermodynamics could be bridged with quantum mechanics. Such computations were made in Chapter 4. On the one hand, ν_{rad} (or λ_{rad}, due to the relation $\nu_{rad} \cdot \lambda_{rad} = c_{light}$) was predetermined in the form of the λ_{rad} value, which had been estimated in [7], namely 1.9 µm. It yielded an A-value of 0.0327×10^{-10} m = 5.8% of R_0.

On the other hand, the *theorem of conservation of momentum* $\boldsymbol{P}$ was applied to the collision process which occurs according to the kinetic gas theory, *i.e.* to the transfer of atomic motion (velocity w) to electronic motion (velocity u), expressed by Equation (27):

$$\boldsymbol{P}_{electron} = m_e \cdot u_{osc} = \overline{\boldsymbol{P}}_{atom} = m_{\mathrm{He}} \cdot \Delta\overline{w}_{\mathrm{He}} \rightarrow u_{osc} = \frac{m_{\mathrm{He}}}{m_e} \cdot \Delta\overline{w}_{\mathrm{He}} \tag{27}$$

The calculation yielded the values $A = 0.0355 \times 10^{-10}$ m and $E_{osc} = 0.121 \times 10^{-18}$ J, which correspond to $\nu_{rad} = 1.83 \times 10^{14}$ s^{-1} and to $\lambda_{rad} = 1.67$ μm, being very close to the estimated value of 1.9 μm. Thus, the here used modelling method was validated in principle.

Finally, in Chapter 5, the asymmetric parts of the oscillator were computed, regarding the condition that the total outer and inner energies must be equal. For $\Delta R_{max,in}$ and $\Delta R_{max,out}$, the values 0.068×10^{-10} m and 0.1035×10^{-10} m were obtained. Using these values, the electron orbit in the excited state could be computed and compared to that in the ground state (**Figure 15(b)** and **Figure 15(a)**). They resembled the elliptic orbit shown in **Figure 10** and thus confirmed this approach, too.

The essential difference between the orthodox and the alternative model consists in the fact that the orthodox model only considers the observer's point of view, whereas the alternative model distinguishes between object and observer. Thereby, the isolated model is two-dimensional, obeying strict quantum-mechanical regularities. However, from the viewpoint of the observer, it appears three-dimensional, since it rotates as a whole due to heat-induced movement, and thus obeys stochastic regularities. But the nucleus/electron distances are not identical: while this distance varies in the orthodox model—even in the ground state—it is constant and well-defined in the alternative model. As a consequence, the alternative model allows computing the electron oscillation, due to the well-defined electron radius, whereas the orthodox model would be unable to do so in default of a well-defined electron radius.

Acknowledgment

I thank Johan M. van der Wiel, Andreas Rüetschi, Harald von Fellenberg, Emil Roduner and Dieter Meschede for their critical objections.

Conflicts of Interest

The author declares no conflicts of interest regarding the publication of this paper.

References

[1] Stefan, J. (1879) Über die Beziehung zwischen der Wärmestrahlung und der Temperatur. *Sitzungsberichte der Mathematisch-Naturwissenschaftlichen Classe der Kaiserlichen Akademie der Wissenschaften*, **79**, 391-428.

[2] Boltzmann, L. (1884) Ableitung des Stefan'schen Gesetzes, betreffend die Abhängigkeit der Wärmestrahlung von der Temperatur aus der electromagnetischen Lichttheorie. *Annalen der Physik*, **258**, 291-294. https://doi.org/10.1002/andp.18842580616

[3] Dulong, M.M. and Petit, A. (1817) Des Recherches sur la Mesure des Températures et sur les Lois de la communication de la chaleur. *Annales de Chimie et de Physique*, **2**, 225-264, 337-367.

[4] Arrhenius, S. (1896) On the Influence of Carbonic Acid in the Air upon the Temperature of the Ground. *Philosophical Magazine*, **41**, 238-276.

[5] Boeker, E. and Van Grondelle, R. (2011) Environmental Physics. Wiley.

https://doi.org/10.1002/9781119974178

[6] Tyndall, J. (1861) On the Absorption and Radiation of Heat by Gases and Vapours and on the Physical Connection of Radiation, Absorption and Conduction. *Philosophical Magazine*, **22**, 169-194, 273-285.

[7] Allmendinger, T. (2016) The Thermal Behaviour of Gases under the Influence of Infrared-Radiation. *International Journal of Physical Sciences*, **11**, 183-205. https://academicjournals.org/journal/IJPS/article-full-text-pdf/E00ABBF60017

[8] Seim, T.O. and Olsen, B.T. (2020) The Influence of IR Absorption and Backscatter Radiation from CO_2 on Air Temperature during Heating in a Simulated Earth/Atmosphere Experiment. *Atmospheric and Climate Sciences*, **10**, 168-185. https://doi.org/10.4236/acs.2020.102009

[9] Crawford, M.F., Welsh, H.L. and Locke, J.L. (1949) Infra-Red Absorption of Oxygen and Nitrogen Induced by Intermolecular Forces. *Physical Review*, **75**, 1607-1607. https://doi.org/10.1103/physrev.75.1607

[10] Frommhold, L. (1994) Collision-Induced Absorption in Gases. Cambridge University Press. https://doi.org/10.1017/cbo9780511524523

[11] Karman, T., Koenis, M.A.J., Banerjee, A., Parker, D.H., Gordon, I.E., van der Avoird, A., *et al.* (2018) O_2-O_2 and O_2-N_2 Collision-Induced Absorption Mechanisms Unravelled. *Nature Chemistry*, **10**, 549-554. https://doi.org/10.1038/s41557-018-0015-x

[12] Allmendinger, T. (2025) A Planar Atom Model of Helium Based on Well-Defined Electron Trajectories. *Journal of Applied Mathematics and Physics*, **13**, 2343-2353. https://doi.org/10.4236/jamp.2025.137133

[13] Allmendinger, T. (2018) The Thermal Radiation of the Atmosphere and Its Role in the So-Called Greenhouse Effect. *Atmospheric and Climate Sciences*, **8**, 212-234. https://doi.org/10.4236/acs.2018.82014

[14] Allmendinger, T. (2016) The Solar-Reflective Characterization of Solid Opaque Materials. *International Journal of Science and Technology Education Research*, **7**, 1-17. https://doi.org/10.5897/ijster2015.0341

[15] Allmendinger, T. (2017) The Refutation of the Climate Greenhouse Theory and a Proposal for a Hopeful Alternative. *Environment Pollution and Climate Change*, **1**, Article 2. https://doi.org/10.4172/2573-458x.1000123